



## EFFECTS OF DAMPER FAILURE ON PERFORMANCE OF A FRAME-CORE TUBE BUILDING UNDER SEVERE EARTHQUAKES

J. Qian<sup>(1)</sup>, Y. Y. Chen<sup>(2)</sup>

<sup>(1)</sup> Professor, Tongji University, jqian@tongji.edu.cn

<sup>(2)</sup> Postgraduate Student, Tongji University, 1530619@tongji.edu.cn

### Abstract

With the development of energy dissipation technology, dampers, as the important energy dissipation components, are getting more applications in the seismic control of high-rise buildings. However, serious damages in dampers have been reported in the recent severe earthquakes, and this puts forward a new challenge toward the performance-based seismic design—the effects of the damper failure on structural performance as an actual event need to be further investigated systematically and thoroughly. The seismic performance of a 30-storey RC frame-core tube building is conducted through the IDA-based seismic fragility analysis. Comparisons are made with cases of all dampers being in effective or destroyed completely. Numerical studies show that the failure of dampers may significantly diminish the resistance capacity and the ductility of the structural system subjected to severe earthquakes, increase the damage probability. And furthermore, with the increase of ground motion intensity, the probability of structural collapse will be accelerated.

*Keywords: energy dissipation; damper failure; seismic fragility; ultimate performance; frame-core tube structure*

### 1. Introduction

During the last 30 years or so, energy dissipation technology has been getting more applications in seismic control of high-rise buildings, in which four kinds of dampers are commonly employed: viscoelastic damper, fluid viscous damper, metal damper and frictional damper<sup>[1]</sup>. Dampers can be installed flexibly in different positions of structures, such as the steel damper installed within replaceable coupling beams<sup>[2]</sup>. Energy dissipation components dissipate the seismic energy to control the seismic responses of structures by self-displacements and self-deformation. Their good performance in seismic control was exhibited in past vibration table tests and earthquakes. However, energy dissipation components encountered unexpected problems in recent severe hazards. Serious damage of oil dampers of a steel building as well as structural destruction in Sendai City in 2011 east Japan earthquake was reported by Xie et al.<sup>[3, 4, 5]</sup>. This event proves that energy dissipation components have their own limit states, indicating that the damper damage puts forward challenges to the safety of high-rise buildings. Therefore, under severe hazards, the damage of energy dissipation components and its effects on ultimate performance of the whole structure deserve further research.

In this work, the effects of failure of steel coupling beam dampers on the seismic performance of a frame-core tube building are studied by comparing two cases in which all dampers being in effective or destroyed completely through IDA-based seismic fragility analysis.

### 2. DAMPER FAILURE

During the field investigation of 2011 Japan earthquake, the Japan Society and Seismic Isolation(JSSI) found that some metal dampers suffered damage to different extent, such as the damper failure due to loosened high-strength connecting bolts and the declination of damper capacity after yielding<sup>[6]</sup>. Meanwhile, according to related mechanical knowledge and tests, steel dampers installed in coupling beams might also suffer the bending failure and shear failure<sup>[7]</sup>.



It is obvious that steel coupling beam dampers might experience various failure modes which haven't been investigated fully and thoroughly. Therefore, in this work, due to the uncertainty of failure modes and distribution of damper failure, we assume that all the dampers are destroyed completely without residual strength in the "damper failure structure" (the structure suffers damper failure). Correspondingly, all the dampers are effective in the "intact structure".

### 3. IDA-BASED SEISMIC FRAGILITY ANALYSIS

Performance-based seismic design (PBSD) approach has achieved a comprehensive theoretical and practical framework which is used to assess the structural performance by analyzing the requirements and seismic capacity of structures under earthquakes of different levels. The main analysis methods are as follows: pushover analysis, multi-mode pushover analysis, nonlinear dynamic analysis, incremental dynamic analysis (IDA), and so on. The IDA method is adopted in this work.

IDA method involves performing a series of nonlinear dynamic analyses under a suite of ground motion records, each scaled to several intensity levels designed to force the structure all the way from elasticity to final global instability<sup>[8,9]</sup>. There are two important parameters in IDA data: an intensity measure (IM) which represents the ground motion intensity level, and a damage measure (DM) which represents the structural response. One can further obtain the seismic fragility curves through probabilistic analysis on IDA data.

Seismic fragility reflects the relationship between ground motion intensity and structural damage degree. In the seismic fragility curves, the horizontal x axis represents ground motion intensity while the vertical y axis represents the exceeding probability of structural responses at a certain performance level. The effects of damper failure are studied in this work by establishing IDA-based seismic fragility curves at different performance levels.

### 4. NUMERICAL RESULTS AND DISCUSSION

In this work, a 30-story reinforced concrete frame-core tube building has been studied, in which the steel dampers are installed in the middle of the coupling beams. The structural configuration, with a plane size of 38.3m×30.8m, is designed based on 9 residential buildings constructed by Shimizu Corporation<sup>[10]</sup> in Japan, as shown in Figures 1a-b. The cross sections of elements are listed in Table 1. The building, reinforced in the software PKPM according to Chinese code GB 50010-2010, has a x-direction first-mode period 2.595s, with its site classified as the III type and second design group of seismic fortification intensity 8(0.2g). The numerical models of two buildings for comparison are built in PERFORM 3D so as to conduct nonlinear time history analysis.

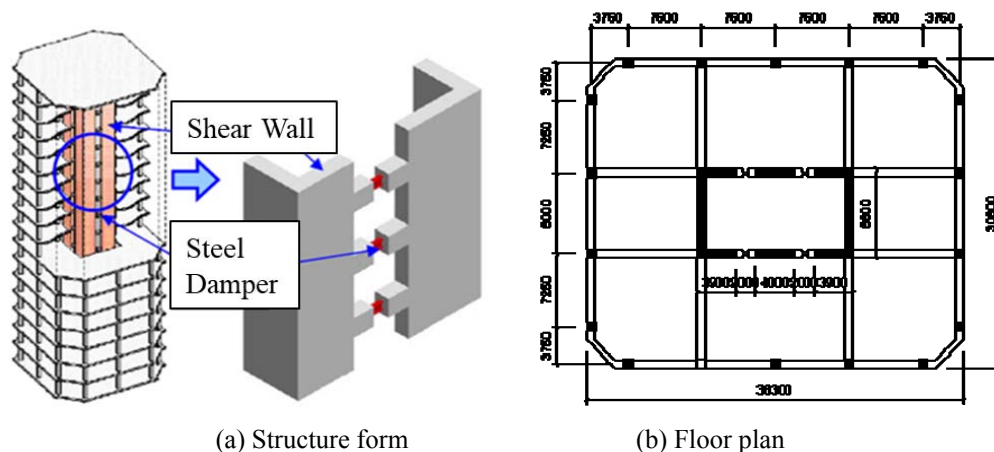


Fig. 1 – Form and layout of the structure



Table 1 – Size information of components

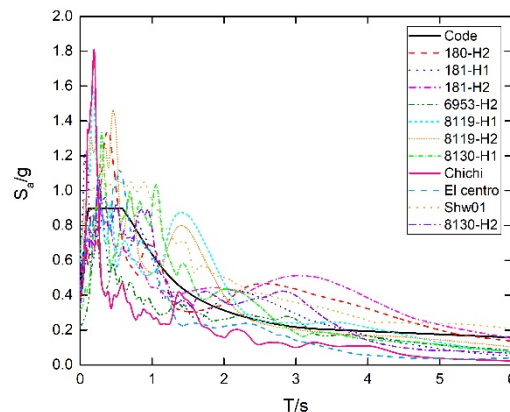
| Wall (mm)        | Column (mm×mm)       | Beam (mm×mm) | Steel damper (I-steel, mm <sup>4</sup> ) |
|------------------|----------------------|--------------|--|
| 1-2 floors 800   | 1-2 floors 900×900   | 400×900      | 200×100×12×12                            |
| 3-11 floors 600  | 3-5 floors 850×850   |              |  |
|                  | 6-11 floors 800×800  |              |  |
| 12-30 floors 400 | 12-14 floors 700×700 |              |  |
|                  | 15-21 floors 650×650 |              |  |
|                  | 22-30 floors 600×600 |              |  |

#### 4.1 Ground Motion Records

Based on the design response spectrum, 11 ground motion records are selected from PEER ground motion database, as the detail information shown in Table 2 and response spectra in Figure 2. The shear wave velocities of selected ground motion records are all about 200m/s due to the site conditions. In order to create obvious structural response, all 11 records have the magnitudes higher than 6.0, the peak ground velocities(PGV) higher than 15m/s, and the peak ground accelerations (PGA) higher than 0.2g. The fault mechanisms of 11 records include strike-slip fault and reversed fault.

Table 2 – Seismic record and the ground motion parameter

| No. | Station            | Name     | Mag  | Vs30(m/s) | PGA(g) | PGV(cm/s) | PGD(cm) | Tg(s) |
|-----|--------------------|----------|------|-----------|--------|-----------|---------|-------|
| 1   | El Centro Array #5 | E05230   | 6.53 | 205.63    | 0.38   | 96.9      | 75.22   | 0.4   |
| 2   | El Centro Array #6 | E06140   | 6.53 | 203.22    | 0.45   | 67.19     | 27.89   | 0.06  |
| 3   | El Centro Array #6 | E06230   | 6.53 | 203.22    | 0.45   | 113.55    | 72.89   | 0.24  |
| 4   | Pages Road Pumping | PRPCS    | 7    | 206       | 0.22   | 56.24     | 48.65   | 0.2   |
| 5   | Pages Road Pumping | PRPCS    | 6.2  | 206       | 0.59   | 81.27     | 38.44   | 0.18  |
| 6   | Pages Road Pumping | PRPCW    | 6.2  | 206       | 0.67   | 96.65     | 40.43   | 0.46  |
| 7   | Shirley Library    | SHLCS40W | 6.2  | 207       | 0.32   | 74.85     | 24.06   | 0.3   |
| 8   | TAP012             | TAP012-E | 7.62 | 207.99    | 0.099  | 18.9      | 14.5    | 0.24  |
| 9   | El Centro Array #9 | ELC180   | 6.95 | 213.44    | 0.28   | 30.94     | 8.66    | 0.5   |
| 10  | Shanghai Wave      | Shw01    | —    | —         | —      | —         | —       | 0.7   |
| 11  | Shirley Library    | SHLCS50E | 6.2  | 207       | 0.34   | 75.35     | 30.47   | 0.26  |

Fig. 2 – Acceleration response spectra of design and the selected earthquake records ( $\beta=0.05$ )



#### 4.2 Incremental Dynamic Analysis(IDA)

IDA for 11 records is conducted in PERFORM 3D. Each beam is simulated by a reinforced concrete section component with two moment hinges at the two ends respectively; each I-section steel damper is simulated by a steel component with a shear hinge in the middle and two moment hinges at the two ends respectively; each column is simulated by a reinforced concrete component with fiber sections at the two ends; each wall is simulated by an inelastic fiber wall component.

The 5% damped first-mode spectral acceleration  $S_a(T_1, 5\%)$  is selected as IM, while the peak interstory drift ratio  $\theta_{max}$  is selected as DM. IM increases in an increment of 0.1g until satisfying the criteria in Han et al. [11]. Postprocessing the obtained discrete IDA points for each record by cubic spline interpolation can generate the IDA curves in Figure 3.

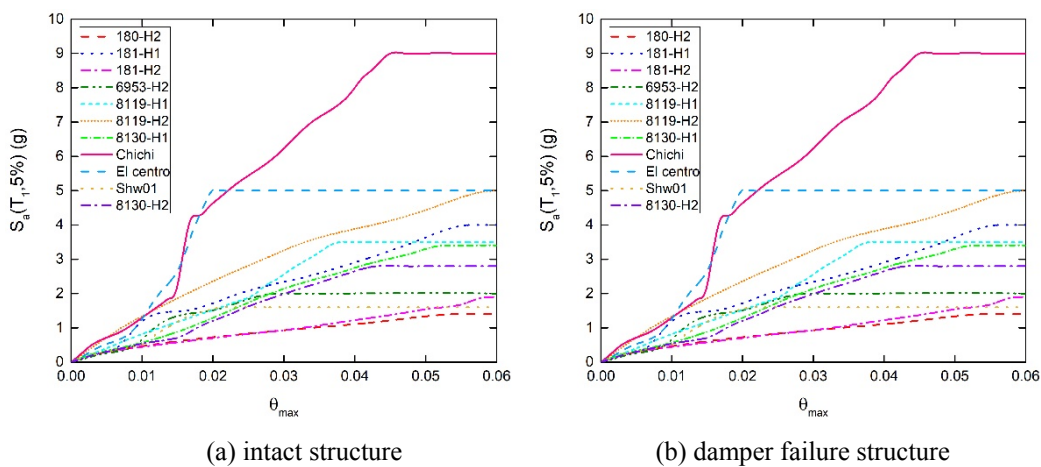


Fig. 3 – IDA curves of the structures

IDA curves are discrete and diverse to some extent. IM-DM relationship can be described as a random function. For any  $DM=f(IM)$ , it is generally assumed that the distribution of DM, with respect to each IM, can be well approximated by a logarithmic normal distribution [12]. Suppose the  $\eta$  and  $\beta$  denote the median and standard deviation for DM respectively when  $IM=x$ , and then the  $\eta \cdot e^{-\beta}$ ,  $\eta$  and  $\eta \cdot e^{\beta}$  denote the 16%, 50% and 84% percentiles for DM respectively. In this way, we can change values of IM and generate the three corresponding percentile IDA curves in Figures 4a-b.

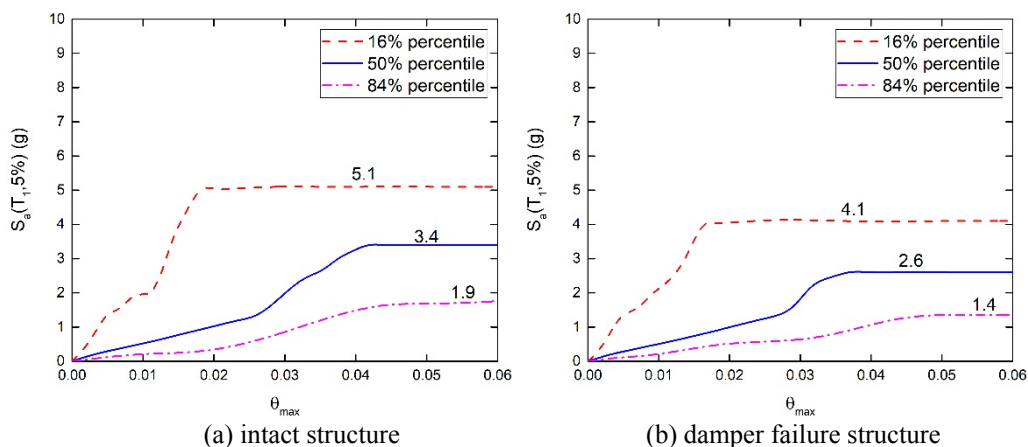


Fig. 4 – IDA percentile curves of the structures



From Figures 4a-b, one can observe that, in each percentile curve, the values of  $S_a(T_1, 5\%)$  with respect to  $\theta_{max}$  of the damper failure structure is lower than that of the intact one, especially when structures reaching the collapse limit state (the platforms in curves). The maximum  $S_a(T_1, 5\%)$  of the intact structure are 5.1g, 3.4g and 1.9g for 16%, 50% and 84% percentiles respectively, while that of the damper failure structure are 4.1g, 2.6g and 1.4g respectively. Therefore, for the three percentile cases, the limit ground motion intensities that the structure can withstand reduce by 19.6%, 23.5% and 26.3% respectively once it suffers damper failure. One can also observe that the damper failure structure reaches its collapse limit state at a smaller  $\theta_{max}$ , 0.036 for 50% percentile compared with that of 0.042 in the intact structure, thus having a worse performance in structural ductility. Therefore, damper failure has obvious negative effects on the performance of structure since it not only decreases the resistant ability against collapsing under extreme earthquake by approximately 20% but also reduces the structural ductility.

#### 4.3 Defining the Limit States

In order to assess the structural performance, 4 limit states are defined according to FEMA365: operational(O), immediate occupancy(IO), life safety(LS) and collapse prevention(CP). For each limit state, a recommended maximum interstory drift ratio  $\theta_{Tds}$  is adopted depending on HAZUS, FEMA<sup>[13]</sup>. The building in this work is classified as C2H-type structure in HAZUS as the description for each limit state shown in Table 3.

Table 3 – Definition of damage state

| Limit State                | CP  | LS   | IO   | O  |
|----------------------------|---|--|--|--|
| Damage Degree              | Very extensive  | Moderate   | Slight   | Very slight  |
| Description                | Structure may have Large permanent lateral displacement or in danger of collapse due to cripple wall failure or failure of lateral resisting system | Large cracks at corners of openings and ceilings; small diagonal cracks across shear wall panels; cracks in foundation | No residual displacements; small cracks at corners of openings and ceilings. | No residual displacements; all components keeping their original stiffness and strength. |
| Recommended $\theta_{max}$ | 0.04  | 0.015  | 0.005  | 0.002  |

#### 4.4 Seismic Fragility Analysis

The seismic fragility of structure can be defined as the probability of structural response DM reaching a certain limit state  $\theta_{Tds}$  under specific ground motion intensity  $IM=x$ , as shown in Eq. (1):

$$F(IM = x) = P[DM > \theta_{Tds} | IM = x] \quad (1)$$

The structural response DM satisfies the logarithmic normal distribution:

$$DM = \text{Lognorm}(\theta_D, \beta_D) \quad (2)$$

Similarly, the distribution of limit state  $T_{ds}$  can be defined as:

$$T_{ds} = \text{Lognorm}(\theta_{Tds}, \beta_{Tds}) \quad (3)$$

Thus, the probability of DM exceeding the  $T_{ds}$  is derived as follows:

$$P[DM > T_{ds} | IM = x] = \Phi \left( -\frac{\ln(\theta_{Tds}) - \ln(\theta_D)}{\sqrt{\beta_{Tds}^2 + \beta_D^2}} \right) \quad (4)$$

The log-linear regression results of IDA data are shown in Figures 5a-b with the expression:

$$\ln(S_a(T_1, 5\%)) = a \ln(\theta_D) + b \quad (5)$$

where  $a$  and  $b$  are equal to 0.9004 and 3.9021 respectively for the damper failure structure, both less than the values of the intact structure, 0.9760 and 4.3294 respectively. With the smaller slope  $a$  and vertical intercept  $b$ , the regression line of the damper failure structure is always underneath that of the intact structure, indicating that, damper failure leads to a decrease of the ground motion intensity level the structure can resist during its whole deformation process.

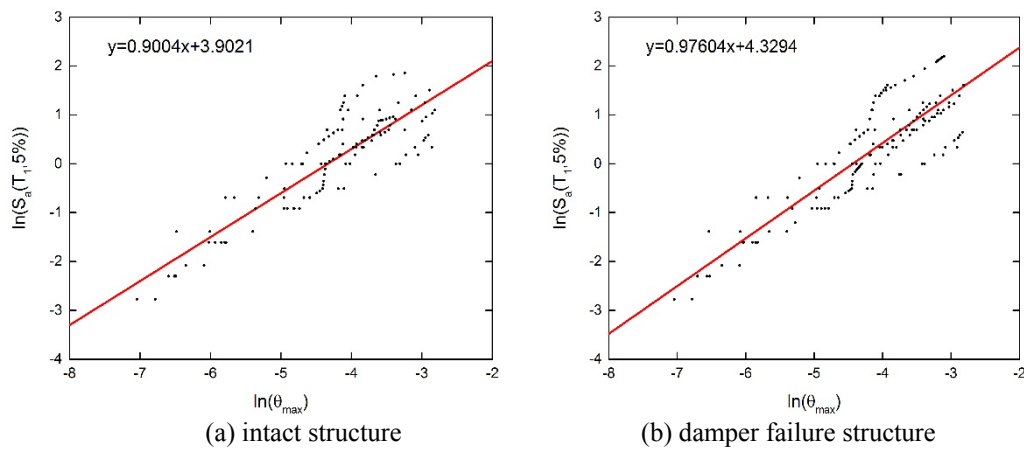


Fig. 5 – Log-linear regression of the IDA data

The recommended value of  $\sqrt{\beta_{Tds}^2 + \beta_D^2}$  is 0.95 according to HAZUS. Submitting Eq. (5) into Eq. (4) can generate the function of damage probability  $P$  versus  $S_a(T_1, 5\%)$ , as plotted in Figure 6. The solid lines represent the intact structure while the dash lines represent the damper failure structure. One can observe that, under the O level, there is little difference between damage probabilities of two structures because the structural responses are very small and still at the elastic stage; but under IO, LS and CP levels the damper failure structure obviously faces a higher damage probability. The more extensive the structural response is, the larger extent to which the damage probability increases. Moreover, under the CP level, the curve slope of damper failure structure stays larger than that of the intact structure, indicating that damper failure accelerates the increase of collapse probability, which increase by 9% when  $S_a(T_1, 5\%)$  is equal to 3g.

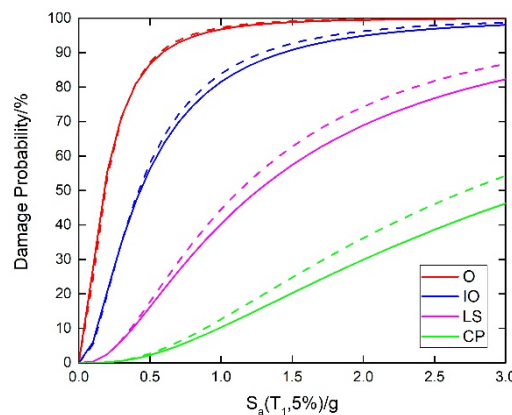


Fig. 6 – Seismic fragility curves of the structures

Note: solid lines represent the intact structure, and dash line represent the damper failure structure.

Under extreme earthquakes, structures usually experience dramatic deformation and are prone to collapse. Therefore, in such cases, the seismic fragility curves of the structures is more likely to be CP level ones, which show obvious increase in the collapse probability when the structure suffers damper failure with an accelerating trend as IM increases.

## 5. CONCLUSION

Energy dissipation structures are getting more successful applications in the aspect of seismic control, the important element of performance-based seismic design (PBSD). However, in recent extreme hazards, the damage and destroy of energy dissipation components were reported, indicating that some recessive effects exist in energy dissipation systems. Therefore, the PBSD method needs to be improved by considering the



effects of damper failure on the performance of structures under extreme loads. A case study of a high-rise building through IDA-based seismic fragility analysis shows that damper failure not only decreases the ultimate ground motion intensity the structure can resist by nearly 20%, but also reduces the structural ductility, increases the structural collapse probability and accelerates the structural collapse. Consequently, the effects of damper failure deserve further research; meanwhile, the residual performance as well as the failure modes of dampers needs to be tested and studied thoroughly.

## 6. Acknowledgements

The authors acknowledge with thanks the support by the National Key Research and Development Program of China (Grant No.2017YFC1500701).

## 7. References

- [1] Lu XL, Jiang HJ (2010): Research progress of earthquake resistance and energy dissipation of complex tall buildings. *Journal of Building Structures*, 31(6), 52-61.
- [2] Lu XL, Chen Y, Jiang HJ (2013): Research progress in new replaceable coupling beams. *Journal of Earthquake Engineering and Engineering Vibration*, 33(1), 8-15.
- [3] Zhou FL, Cui HC, Shigetaka ABE3 et al (2012): Inspection report of the disaster of the East Japan earthquake by Sino-Japanese joint mission. *Building Structure*, 4, 1-20.
- [4] Xie LY, Hao LF, Zhang RF, et al (2015): Performance of Seismic Energy Dissipation Structure in the Great East Japan Earthquake. *Structural Engineers*, 31(2), 10-20.
- [5] Xie LY, Tang HS, Xue ST (2015): Lessons Learned for Design of Passively-controlled Structures from the Great East Japan Earthquake. *Structural Engineers*, 31(2), 2-9.
- [6] Xie LY, Tang HS, Xue ST (2014): State-of-the-art and Future Trend in Limit State and Rehabilitation of Vibration-controlled High-rise Buildings. *Structural Engineers*, 3, 205-212.
- [7] Deng FY, Wang T, Shi W (2016): Cyclic test on seismic behavior of energy-dissipative coupling beams with dampers. *China Civil Engineering Journal*, 49(S1), 96-100, 113.
- [8] Vamvatsikos D, Cornell CA (2004): Applied incremental dynamic analysis. *Earthquake Spectra*, 20(2), 523-553.
- [9] Vamvatsikos D, Fragiadakis M (2010): Incremental dynamic analysis for estimating seismic performance sensitivity and uncertainty. *Earthquake Engineering and Structural Dynamics*, 39(2), 141-163.
- [10] Han JP, Lu XL, Li H (2007): State-of-the-art of performance-based earthquake engineering and need for structural nonlinear analysis. *Journal of Earthquake Engineering and Engineering Vibration*, 27(4), 15-23.
- [11] Hitoshi K (2010): Earthquake Response of a High-Rise Building with Reinforced Concrete Shear Walls and Coupling Beam Dampers. *Shimizu Corporation Report*.
- [12] Lu XL (2015): *Seismic Theory and Application of Complex High-rise Structures*. Science Press.
- [13] Federal Emergency Management Agency (2012): *Advanced Engineering Building Module (AEBM). Technical and User's Manual*.